Published online: June 30, 2017

Article

SOURCE DATA | TRANSPARENT PROCESS

THE EMBO JOURNAL

Structural basis of divergent cyclin-dependent kinase activation by Spy1/RINGO proteins

Denise A McGrath[1], Bre-Anne Fifield[2], Aimee H Marceau[1], Sarvind Tripathi[1], Lisa A Porter[2] & Seth M Rubin[1,*]

Abstract

Cyclin-dependent kinases (Cdks) are principal drivers of cell division and are an important therapeutic target to inhibit aberrant proliferation. Cdk enzymatic activity is tightly controlled through cyclin interactions, posttranslational modifications, and binding of inhibitors such as the p27 tumor suppressor protein. Spy1/RINGO (Spy1) proteins bind and activate Cdk but are resistant to canonical regulatory mechanisms that establish cell-cycle checkpoints. Cancer cells exploit Spy1 to stimulate proliferation through inappropriate activation of Cdks, yet the mechanism is unknown. We have determined crystal structures of the Cdk2-Spy1 and p27-Cdk2-Spy1 complexes that reveal how Spy1 activates Cdk. We find that Spy1 confers structural changes to Cdk2 that obviate the requirement of Cdk activation loop phosphorylation. Spy1 lacks the cyclin-binding site that mediates p27 and substrate affinity, explaining why Cdk-Spy1 is poorly inhibited by p27 and lacks specificity for substrates with cyclin-docking sites. We identify mutations in Spy1 that ablate its ability to activate Cdk2 and to proliferate cells. Our structural description of Spy1 provides important mechanistic insights that may be utilized for targeting upregulated Spy1 in cancer.

Keywords Cdk; cell cycle; kinase inhibitors; p27; protein phosphorylation
Subject Categories Cell Cycle; Structural Biology
DOI 10.15252/embj.201796905 | Received 9 March 2017 | Revised 27 May 2017 | Accepted 2 June 2017

Introduction

Cyclin-dependent kinases (Cdks) are central cell-cycle regulatory enzymes that control cell fate decisions through phosphorylation of numerous protein substrates (Morgan, 2007). Cdks stimulate cell-cycle progression in normal and cancer cells and are a promising therapeutic target for halting cell proliferation (Stone *et al*, 2012; O'Leary *et al*, 2016). Cdk activity is regulated by several mechanisms that are critical for the intrinsic oscillations of the cell cycle and response of the cell cycle to external inputs such as growth factor signaling (Morgan, 2007). Typically, the Cdk catalytic domain remains inactive until bound by the cyclin subunit, and other kinases phosphorylate Cdk to stimulate further its enzymatic activity. Cdk activity can also be inhibited through the direct binding to Cdk inhibitor proteins that either prevent Cdk-cyclin assembly or form a ternary repressed complex. Tumor cells acquire genetic changes that bypass Cdk inhibition either by upregulating cyclin levels or downregulating Cdk inhibitor levels (Sherr, 1996; Kim & Sharpless, 2006; Malumbres & Barbacid, 2009). In addition, several viruses have co-opted cyclins to inappropriately drive host cell proliferation (Swanton *et al*, 1997).

Several noncanonical (i.e., non-cyclin) protein regulators of Cdk activity play important roles in normal and cancer cell growth (Nebreda, 2006). Here we focus on the structure and activity of the Cdk regulator known as Speedy (Spy1; also known as RINGO) (Ferby *et al*, 1999; Lenormand *et al*, 1999; Porter *et al*, 2002). There are five known mammalian Spy1 paralogs, which are all highly expressed in the testes (Cheng *et al*, 2005b; Dinarina *et al*, 2005). Speedy A (Spy1A, herein referred to as Spy1) is the best characterized and the only isoform that is ubiquitously expressed in somatic tissues (Porter *et al*, 2002). The physiological roles of Spy1 proteins are just beginning to be uncovered. Spy1 is critical for meiosis in both egg and sperm (Ferby *et al*, 1999; Porter *et al*, 2002; Cheng *et al*, 2005b; Mikolcevic *et al*, 2016). Expression of non-degradable forms of Spy1 induces unregulated cell proliferation and oncogenic properties (Al Sorkhy *et al*, 2009), and Spy1 overexpression is implicated in the initiation of tumorigenesis (Ferby *et al*, 1999; Porter *et al*, 2002; Cheng *et al*, 2005b; Golipour *et al*, 2008; Mikolcevic *et al*, 2016).

Spy1 proteins share no significant sequence homology with cyclins (Fig EV1). All Spy1 paralogs contain a highly conserved domain of about 130 amino acids called the Speedy/Ringo box (S/R box), which is required for Cdk binding and activation (Cheng *et al*, 2005b; Dinarina *et al*, 2005). Spy1 can directly bind and activate both Cdk1 and Cdk2, and Spy1 overexpression induces cells to progress faster through the cell cycle and to override checkpoints (Barnes *et al*, 2003; Gastwirt *et al*, 2006; McAndrew *et al*, 2009).

An important difference between Spy1 and classical cyclin proteins is that Cdk-Spy1 activity is refractory to the well-characterized mechanisms that regulate Cdk-cyclin activity. For example, unlike Cdk-cyclins, Cdk-Spy1 does not require the positive input of

1 Department of Chemistry and Biochemistry, University of California, Santa Cruz, CA, USA
2 Department of Biological Sciences, University of Windsor, Windsor, ON, Canada
*Corresponding author. Tel: +1 831 459 1921; E-mail: srubin@ucsc.edu

Cdk-activating kinase (CAK) for activity, and Spy1-bound Cdk2 is not inhibited by the Cdk inhibitors p21 or p27 (Karaiskou *et al*, 2001; Cheng *et al*, 2005a; Al Sorkhy *et al*, 2016). Spy1 also confers expanded specificity to Cdk (Cheng *et al*, 2005a), implying that Spy1-bound Cdk can target noncanonical Cdk substrates. Therefore, Spy1 is a potent Cdk activator whose expression overrides normal cell-cycle signaling inputs that control Cdk function. Whether there is reduced access of Cdk inhibitors to the Cdk active site and whether Spy1-bound Cdks assume a different conformation have never been resolved.

We have determined the first structures of Spy1 that explain how Spy1 activates Cdk to stimulate cell-cycle progression. We find that despite its low sequence homology with cyclin, Spy1 adopts a cyclin fold that binds and induces an active Cdk conformation. The structure and biochemical analysis reveal how Spy1 coordinates the Cdk activation loop independent of CAK phosphorylation. We also find that Spy1 lacks a binding site for p27 and substrates, which results in weak Cdk-Spy1 inhibition and a lack of preference for substrates containing canonical cyclin-docking sites. Our work explains why cancer cells may upregulate Spy1 as a Cdk activator that is refractory to protective cell-cycle checkpoint mechanisms.

Results

Spy1 contains a cyclin fold that binds Cdk2 and induces its active conformation

We grew crystals and solved the 2.7 Å structure of human Cdk2 bound to a construct from human Spy1A (residues 61–213) corresponding to the S/R box (Cheng *et al*, 2005a; Karaiskou *et al*, 2001; Table EV1 and Fig 1). Cdk2 and the S/R box form a stoichiometric heterodimer, and there is one complex in the crystal asymmetric unit. Cdk2 has the bi-lobal structure typical of protein kinases. The Cdk2 N-terminal domain contains a beta sheet and the PSTAIRE activation helix (called C-helix in other kinases), while the C-terminal domain is helical and contains the T-loop (activation loop). The structure of Cdk2 in the complex is similar to structures of Cdk2 bound by cyclin A (CycA) (Fig 1B) (Jeffrey *et al*, 1995; Russo *et al*, 1996a,b). The PSTAIRE helix is pushed in toward the center of the N-lobe with E51 pointing toward the active site (Fig 1A). The T-loop contacts Spy1 and is pulled ~5–6 Å away from the active site relative to its position in the structure of Cdk2 alone. These PSTAIRE and T-loop conformations are associated with active kinase, which supports and explains previous findings that Spy1 can substitute for a canonical cyclin in stimulating Cdk activity (Karaiskou *et al*, 2001; Porter *et al*, 2002; Cheng *et al*, 2005a).

The S/R box structure, despite its low sequence homology with cyclin proteins (Fig EV1), has a cyclin box fold (CBF), which consists of a five-helix bundle arranged with four helices (α1, α2, α4, α5) surrounding a central helix (α3) (Fig 1C and D) (Noble *et al*, 1997). The S/R box contains one additional helix N-terminal to the CBF (α1′) and two short helices C-terminal to the CBF (α6 and α7). Unlike the canonical Cdk-activating cyclins, Spy1 contains only a single CBF. It binds Cdk2 in the same position as the N-terminal CBF of CycA (Jeffrey *et al*, 1995). Spy1 α3, α5, the α3–α4 loop, and the α5–α6 loop contact the PSTAIRE helix in Cdk2, while Spy1 α2, the α3–α4 loop, α6, and the loop that follows α7 bind and position the Cdk2 T-loop.

The most extensive interface between Spy1 and Cdk2 occurs between the PSTAIRE helix and helices α3 the α5 of Spy1 (Figs 1C and D, and 2). The interface consists of several hydrogen bonds involving charged side chains (Fig 2A). For example, R164 and D165 in α5 of Spy1 hydrogen bond with backbone atoms in the loop just N-terminal to the PSTAIRE helix, and the C-terminus of the PSTAIRE helix is bound through hydrogen bonds involving D172 and R174 in Spy1. Cdk2 R50, which is in the center of the PSTAIRE helix, makes a number of hydrogen bonds with the C-terminus of the Spy1 α3 helix and D136 in the α3–α4 loop. The PSTAIRE-Spy1 interface is also stabilized by a group of hydrophobic residues in Cdk2 consisting of V44, I49, and I52. Speedy inserts W168 and Y173 into this hydrophobic patch, and the indole nitrogen of W168 forms a hydrogen bond with S53 of Cdk2 (Fig 2A).

The S/R box secondary structural elements at the PSTAIRE interface align with CycA (Fig 1C), and several hydrogen bond contacts between the PSTAIRE helix and Spy1 are similar to those present in the Cdk2-CycA structure (Jeffrey *et al*, 1995). In contrast, the PSTAIRE hydrophobic patch is engaged differently by CycA. Whereas Spy1 primarily uses W168, CycA uses F304 and L299. These differences exemplify how the remarkably divergent sequences among Cdk activators still converge on structures that induce the kinase into its active conformation. It is noteworthy that many residues in Spy1 that contact the PSTAIRE helix are not strictly conserved between the Spy1 paralogs (Fig 1D). For example, few residues in α5 and the α5–α6 loop are conserved, and there are differences in the size of hydrophobic side chains at several positions including at W168. This variation within the Spy1 family suggests that this interface is pliable and that the PSTAIRE helix is engaged and positioned in subtly different ways.

Spy1 binding induces an active Cdk T-loop conformation

It has previously been observed that human *Xenopus* Spy1/RINGO can increase the extent of histone peptide phosphorylation by Cdk1 or Cdk2 and that this activity does not depend on activity of the upstream CAK (Karaiskou *et al*, 2001; Cheng *et al*, 2005a). Our structure of Cdk2-Spy1 reveals that the Spy1 S/R box contacts the T-loop and draws it away from the kinase domain (Fig 1C). Cyclin binding pulls the T-loop out of the active site to some extent (Fig 1C) as observed in comparing the structures of Cdk2-CycA and Cdk2 alone (Debondt *et al*, 1993; Jeffrey *et al*, 1995; Russo *et al*, 1996b). However, until T160 is phosphorylated, T160 and its adjacent residues still partially occlude the substrate-binding site (Fig 3A). Insofar that it is completely removed from the substrate cleft, the unphosphorylated T-loop conformation in Cdk2 bound to Spy1 more closely resembles the conformation of the T-loop when Cdk2 is bound to CycA and phosphorylated on T160 (Fig 3A).

These structural data support the hypothesis that Spy1 can stimulate Cdk activity by inducing a completely active T-loop structure, and therefore, Cdk2-Spy1 activity does not depend on whether T160 is phosphorylated by CAK. To further test this idea and quantitatively measure Cdk-Spy1 kinetics toward cell-cycle substrates, we measured steady-state phosphorylation rates of Cdk2-Spy1 toward protein fragments of FoxM1 (Fig 3B and C) and the retinoblastoma protein (Rb) (Fig EV2). We purified recombinant human FoxM1B (hereafter called FoxM1) residues 526–748, which corresponds to a

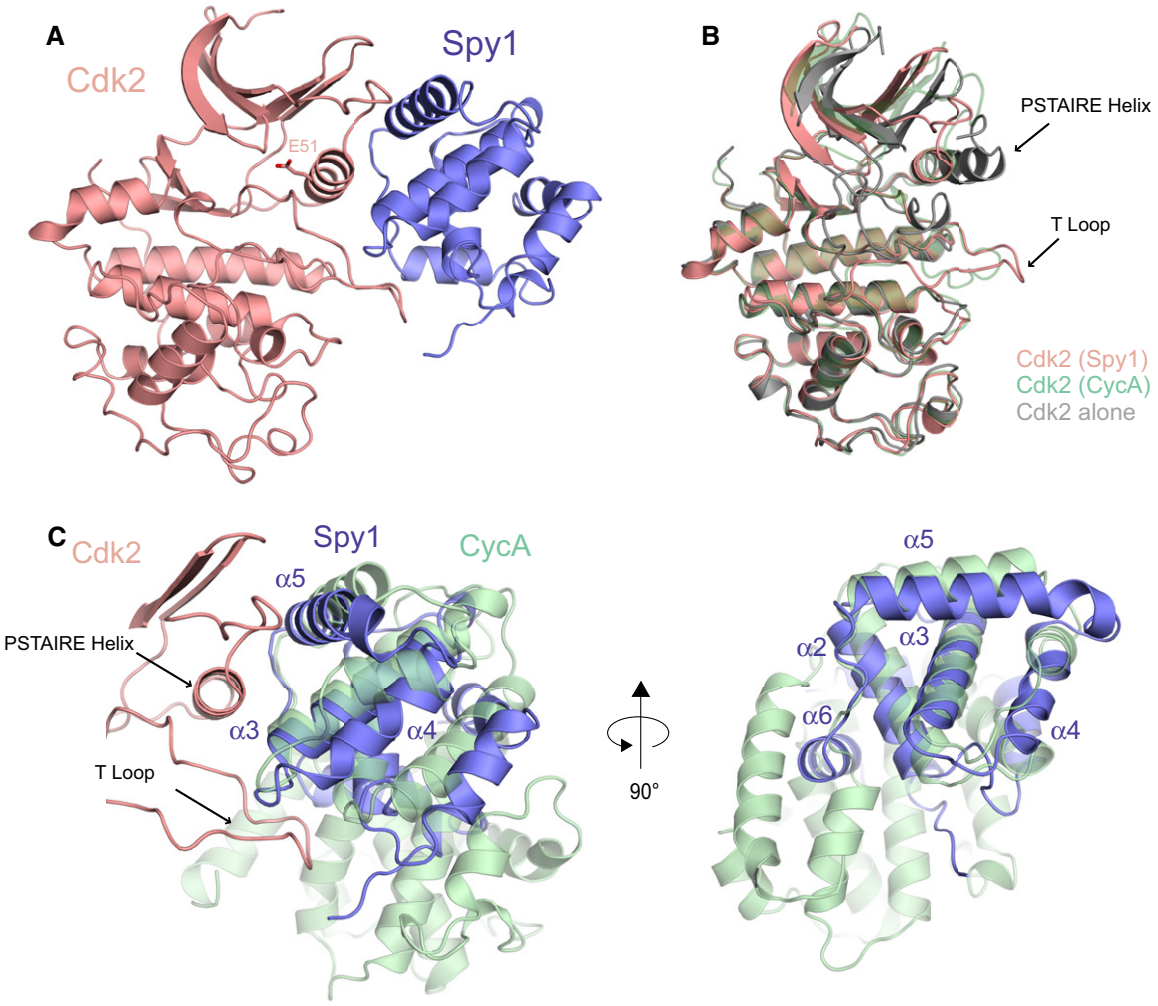

D

```
                                α1'      α1          α2                  α3          α4
                                         81         101                121         141
hs Spy1A    61 GPCLV--IQRQDMTAFFKLFDDDLIQDFLWMDCCCKIADKYLLAMTFVYFKRAKFTISEHTRINFFIALYLANTVEEDEEETKYEIFPWALG
hs Spy1C    62 GNGFLRFRQHQEVQAFLSLLEDSFVQEFLSKDPCFQISDKYLLAMVLVYFQRAHLKLSEYTHSSLFLALYLANDMEEDLEGPKCEIFPWALG
hs Spy1E4   96 KRASS--VLPEHHEAFNRLLGDPVVQKFLAWDKDLRVSDKYLLAMVIAYFSRAGLFSWQYQRIHFFLALYLASDMEEDNQAPKQDIFSFLYG
mm Spy1B  127 RRVST--VRPEHHKVFTKLLEDPVVKKFLTWDKMLRVSDKYLLSMVIAYFSRAGLFSWQYRPIHFFLALYLANDMEEDNQAPKQDIFYFLYG
mm Spy1D  196 KRRAS--YRPEDLEAFYRLLEDPVVQNFLAADIFFRVTDKYLLSMVVEYFGRVGLPGHLYNRIYFFLALYIACDMEEDDPISKRSIFQFLLG
xl Spy1    54 ITHLN--LQPQERQAFYRLLENELIQEFLSMDSCLKISDKYLIAMVLAYFKRAGLYTGEYTTMNFFVALYLANDMEEDEEDYKYEIFPWALG

                                α5          α6          α7
                                161        181         201
hs Spy1A   151 KNWRK-LFPNFLKLRDQLWDRIDYRAIVSRRCCEEVMAIAPTHYIWQRERSVHHSGAVRNYNR 212
hs Spy1C   154 KDWCL-RVGKFLHQRDKLWARMGFRAVVSRQCCEEVMAKEPFHWAWTRDRRPHHGGVQRVCPQ 215
hs Spy1E4  186 KNYSQ--RPLFHKLRYQLLCSMRWRTWVSPEEMEEIQAYDPEHWVWARDRTLIS           237
mm Spy1B   218 KSYAQ--RPMFHKLRFQFIRSMGWKIWVSREECEEIQAYNPDLWVWARDRTNLT           269
mm Spy1D   286 RDTWQGLYKDFLKLQKDFILAMDYQAWVTPDQCAEIQNQNPQHWVWSRVRQGTP           339
xl Spy1    144 DSWRE-FFPQFLRLRDNFWAKMNYRAVVSRRCCDEVMAKDPTHWAWLRDRPIHHSGALRGYLR 205
```

Figure 1. Spy1 binding induces an active Cdk2 conformation.

A Overall structure of the Cdk2-Spy1 (S/R box) complex.

B Comparison of kinase domain structures between Cdk2 alone and Cdk2 in complex with CycA or Spy1. The conformation of the PSTAIRE helix (E51 pointed toward the active site) and T-loop (extended away from the active site) in the Spy1 complex are similar to their conformations in the active CycA complex.

C Comparison of CycA and Spy1 bound to Cdk2 generated by alignment of the kinase domain in the two complex structures. Spy has a single cyclin box fold, and the helices that contact the PSTAIRE helix have similar position and orientation to the analogous helices in CycA.

D Sequence alignment of Spy1 homologs within the S/R box domain. Secondary structures from the Cdk2-Spy1A structure are shown, with dashed lines corresponding to sequences for which there was no observable electron density. Residues in Spy1 that contact the Cdk2 PSTAIRE helix (red squares) and T-loop (red circles) are indicated.

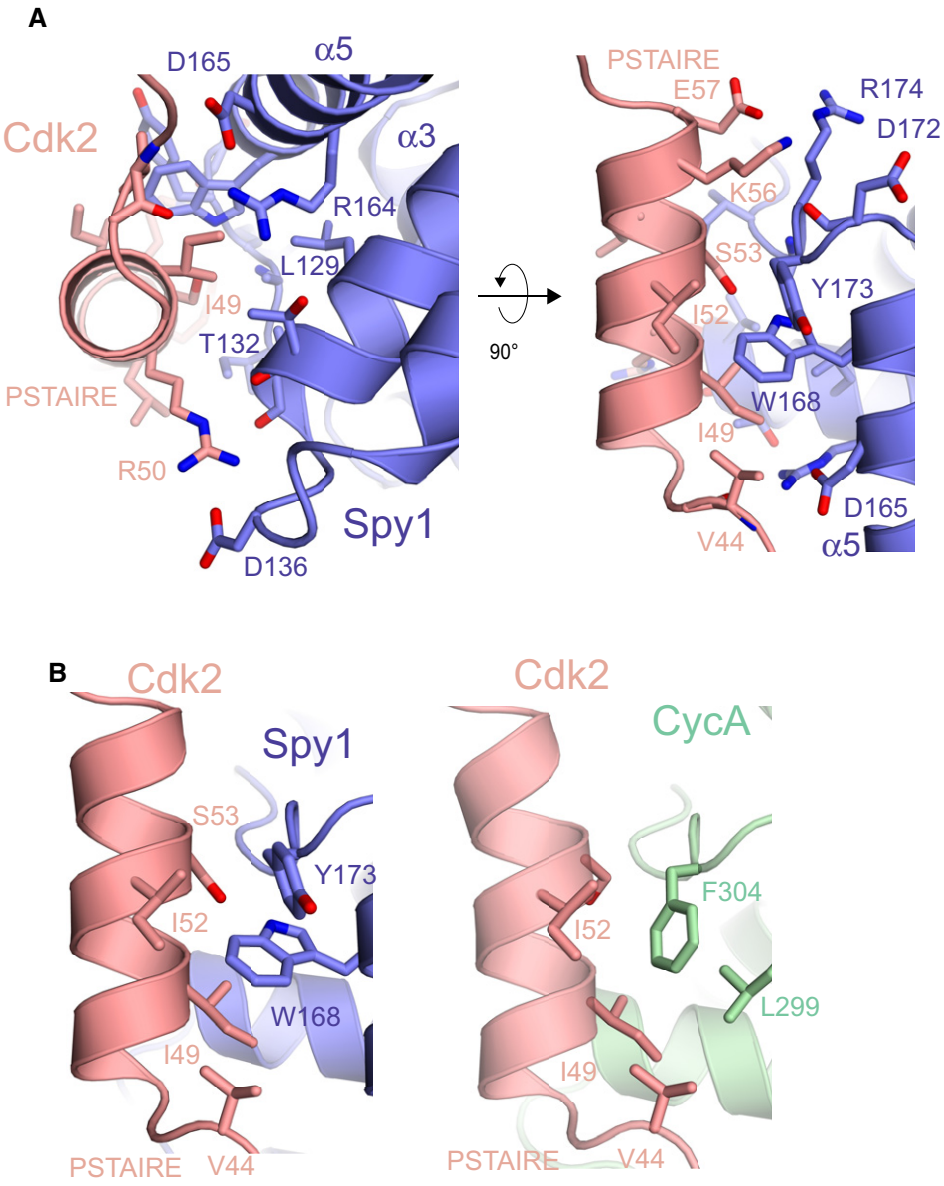

Figure 2. Spy1 interactions with the Cdk2 PSTAIRE helix.

A Close-up view of the Spy1-PSTAIRE interface.

B Comparison of PSTAIRE helix interactions between Spy1 and CycA.

predicted disordered region of the protein and contains five consensus Cdk sites that are important for FoxM1 activation and mitotic gene expression (Major *et al*, 2004; Laoukili *et al*, 2008). We phosphorylated this fragment with ^{32}P-labeled ATP in reactions containing Cdk2-CycA, Cdk2-Spy1 (S/R box domain), and both kinase complexes phosphorylated by CAK (phosCdk2-CycA and phosCdk2-Spy1). We assayed the rate of phosphate incorporation as a function of FoxM1 concentration by measuring SDS–PAGE band intensity after phosphorimaging. Consistent with previous assays using other substrates (Karaiskou *et al*, 2001; Cheng *et al*, 2005a), we find that phosphorylation of Cdk2-CycA leads to a twofold decrease in K_M (Michaelis constant) and a 25-fold increase in the maximum initial rate (V_{max}). In contrast, both unphosphorylated and phosphorylated Cdk2-Spy1 have similar K_M and V_{max} values, with the V_{max} falling between unphosphorylated and phosphorylated Cdk2-CycA. We found similar results phosphorylating the C-terminal domain of the retinoblastoma protein (Fig EV2).

The structural details at the Cdk2-Spy1 interface explain how Spy1 is able to induce the active T-loop conformation (Fig 4A). The interface is composed primarily of hydrogen bond and electrostatic interactions. Several interactions are made by three consecutive acidic residues (E134, E135, and D136) in the Spy1 α3–α4 loop, which inserts between the Cdk2 PSTAIRE helix and T-loop. Spy1 D136 coordinates three arginines in Cdk2, including one from the

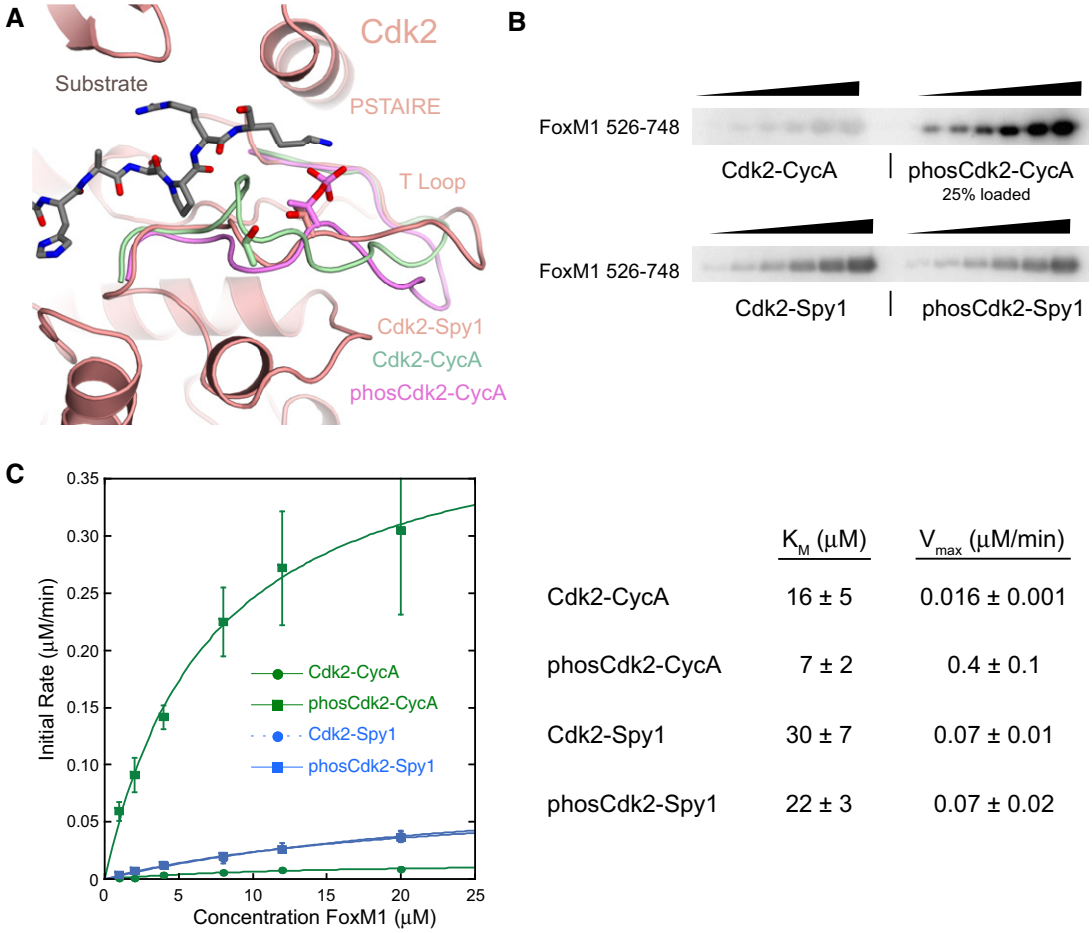

	K_M (µM)	V_{max} (µM/min)
Cdk2-CycA	16 ± 5	0.016 ± 0.001
phosCdk2-CycA	7 ± 2	0.4 ± 0.1
Cdk2-Spy1	30 ± 7	0.07 ± 0.01
phosCdk2-Spy1	22 ± 3	0.07 ± 0.02

Figure 3. Cdk2-Spy1 activity is insensitive to Cdk2 T-loop phosphorylation.

A Comparison of T-loop conformations in the indicated Cdk2 complexes. Spy1 induces a T-loop structure that is more similar to the active conformation in phosphorylated Cdk2. The position of the T-loop T160 is shown in each structure.

B Radiolabeled phosphate incorporation into increasing amounts of FoxM1 substrate by the indicated kinase complex in a 10-min reaction with ^{32}P-ATP. The lanes correspond to 1, 2, 4, 8, 12, and 20 µM FoxM1. The assay was performed with Cdk2-CycA and Cdk2-Spy1 S/R box.

C Initial kinase reaction rates determined from quantification of bands in experiments as in (B). Reported values are averages from three different experiments with the standard deviations shown as error bars. The kinetic parameters (with standard deviations reported as errors) averaged over the three replicates are shown in the table.

Source data are available online for this figure.

PSTAIRE helix (R50) and one from the T-loop (R150). This position of D136 is analogous to the position of the T160 side chain phosphate in the phosCdk2-CycA structure (Russo *et al*, 1996b), and the phosphate similarly coordinates the arginine triad. Although T160 is unphosphorylated in the Cdk2-Spy1 complex, Spy1 D136 also hydrogen bonds with the Cdk T160 peptide amine such that the T160 location is identical to that of phosphorylated T160 in the phosCdk2-CycA structure. Spy1 further pulls the T-loop out from the substrate cleft through interactions with residues that are just N-terminal to T160. Spy1 E135 hydrogen bonds with the side chain oxygen and peptide amide of Cdk2 T158, and Spy1 D97 forms a salt bridge with Cdk R157. Both of these interactions have no analogy in the Cdk2-CycA structures. In contrast to the Spy1 residues that contact the PSTAIRE helix, the Spy1 residues that bind the T-loop are highly conserved among Spy1 paralogs (Fig 1C). This strict conservation suggests that that proper T-loop positioning is a critical aspect of Spy1-induced activation of Cdk.

Mutation of T-loop-binding residues inactivate Spy1

We tested using the phosphorylation assay the prediction from the structure that the interactions made by D97 and E135 with the T-loop are critical for Cdk2 activation by Spy1. We expressed and purified a full-length D97N/E135Q Spy1 mutant (Spy1-DE) and found that it showed no activity toward FoxM1 (Fig 4B) or Rb (Fig EV2). Previous data support that the proliferative effects of Spy1 are dependent on activation of Cdk2 (Porter *et al*, 2002). Using cell lines and conditions previously used to study this Spy1 activity, we tested if the Spy1-DE mutant would retain the proliferative capabilities of Spy1 wild type. Spy1-DE or wild-type plasmids were

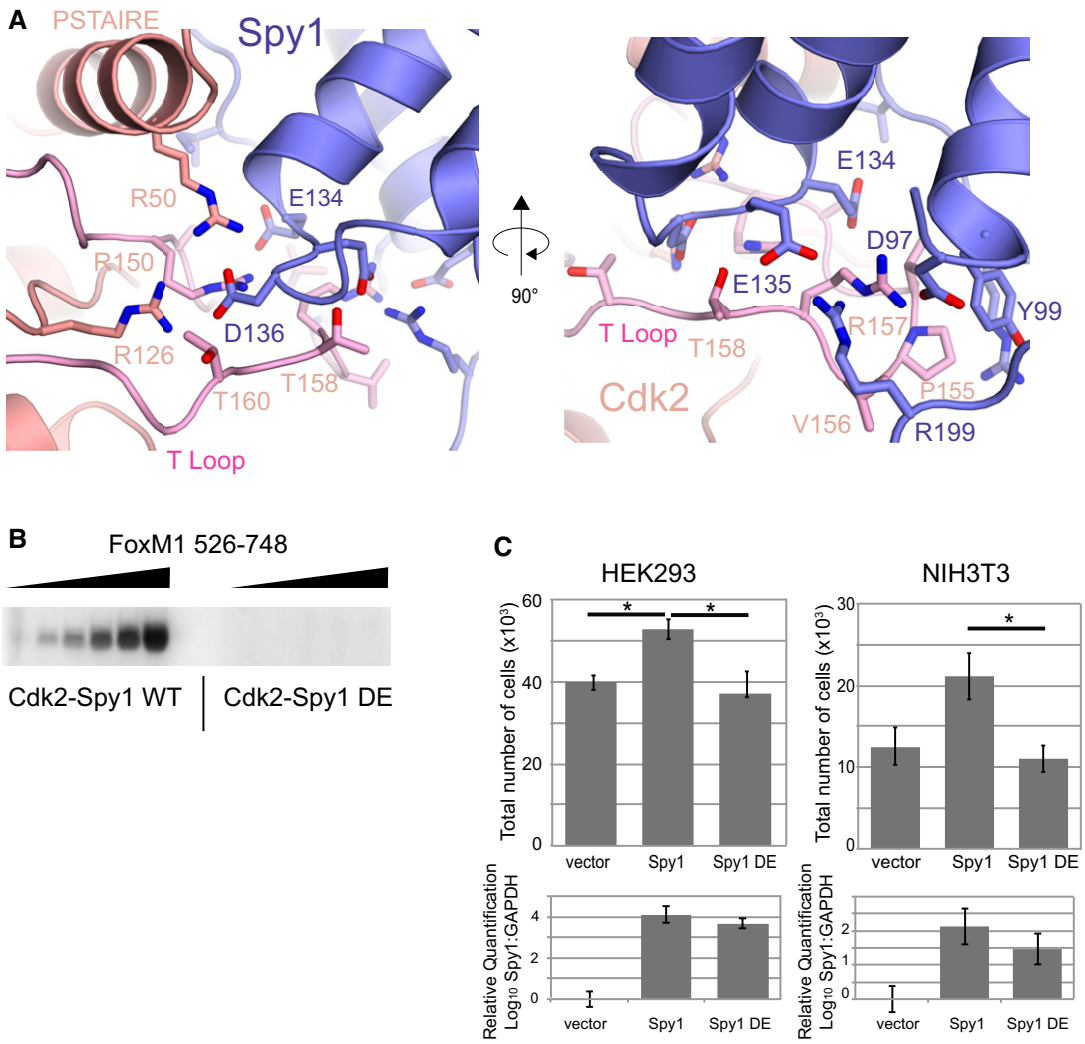

Figure 4. Spy1 coordinates the Cdk2 T-loop using several conserved acidic side chains.

A Close-up view of the Spy1 interface with the Cdk2 T-loop.

B Mutation of D97 and E135 in full-length Spy1 (Spy1 DE) abrogates kinase activity as observed in the same assay described in Fig 3B.

C HEK-293 and NIH 3T3 cells were transiently transfected with empty vector control (vector), Spy1 wild type (Spy1) or Spy1-DE (Spy1 DE) and RT–qPCR was used to confirm transfection and monitor expression levels (bottom graphs). Trypan blue exclusion analysis was used to assess proliferation after 5 days (top graphs). Error bars represent standard error (n = 3); Student's t-test; *$P < 0.05$.

Source data are available online for this figure.

expressed in HEK-293 and NIH 3T3 cells and cell proliferation was monitored over 5 days (Fig 4C). Mutation of D97 and E135 in the T-loop of the DE mutant abrogated the ability of Spy1 to proliferate cells.

Spy1 lacks the canonical cyclin-binding cleft for protein inhibitors

In addition to activating Cdk through structural reorganization of the kinase domain, cyclin proteins regulate Cdk activity through binding substrates and members of the Kip family of protein inhibitors including p27 (Sherr & Roberts, 1995; Russo *et al*, 1996a; Schulman *et al*, 1998; Brown *et al*, 1999). Kip proteins and substrates use a (K/R)xLF or (K/R)xLxF sequence motif that docks into a cleft formed between helices α1 and α3 of the cyclin N-terminal CBF (Russo *et al*, 1996a; Brown *et al*, 1999). The cleft is called the MRAIL site, because of the cyclin sequence in α1 at the site. Notably, the MRAIL sequence is missing in Spy1, and the docking cleft is not present in the Cdk2-Spy1 structure (Fig 5A). The α1 and α3 helices are shorter in Spy1 and lack pockets for binding the consensus leucine or phenylalanine in the Kip/substrate motif (e.g., L32 and F33 in p27). Moreover, the interactions between the α1 and α3 helices position side chains (such as L82 and W147 in Spy1) to occlude the p27-docking surface.

While Spy1 association with p27 has been detected in cells, Spy1 expression overcomes a p27 induced cell arrest, and Spy1 induces Cdk2 activity in lysates in the presence of p27 (Porter *et al*, 2003; McAndrew *et al*, 2007; Al Sorkhy *et al*, 2016). Our structural data

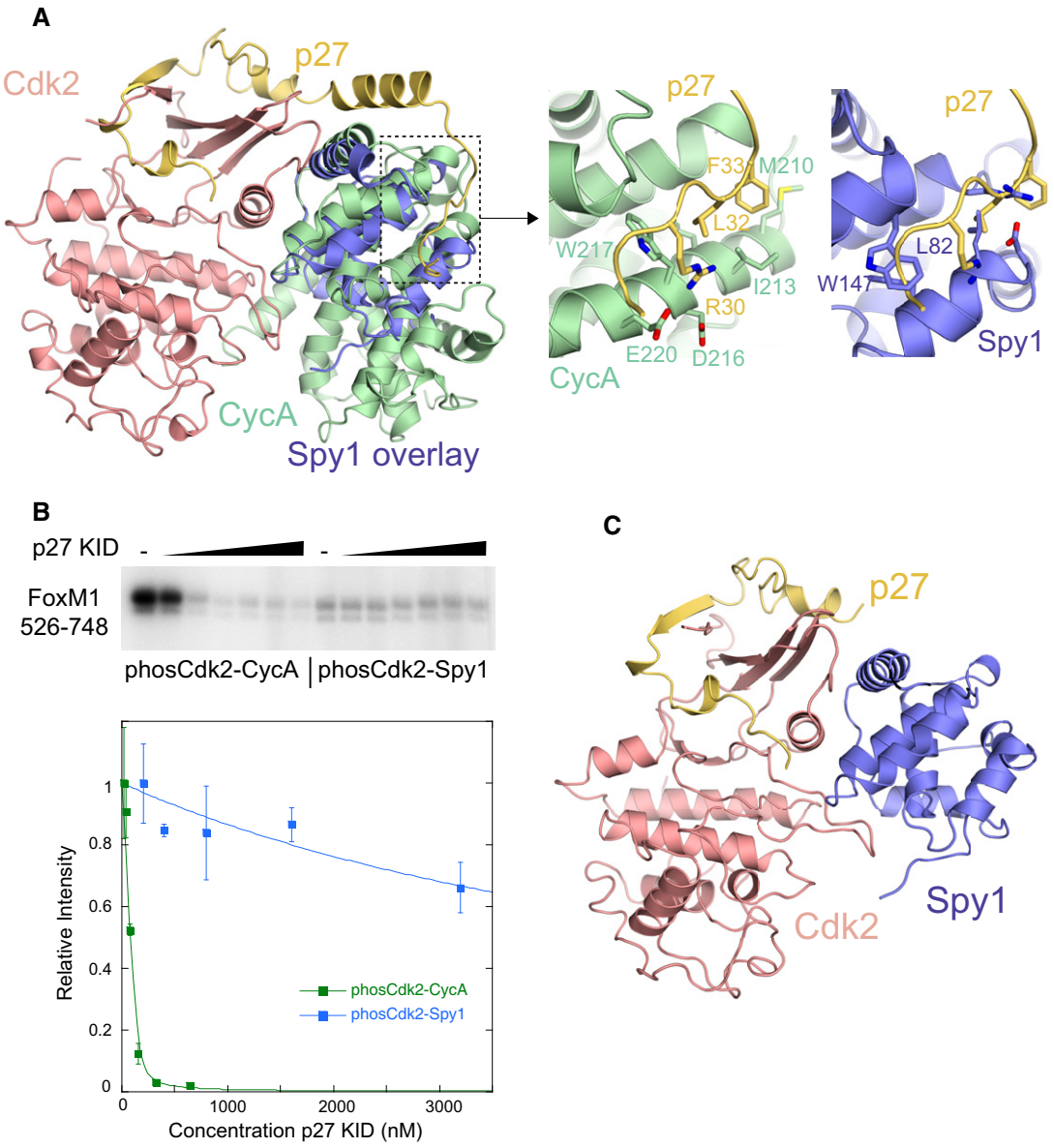

Figure 5. Spy1 lacks the binding cleft for Cdk inhibitors and substrates.

A Comparison of CycA and Spy1 generated by alignment of the Cdk2 kinase domains in the Cdk2-Spy1 and Cdk2-CycA-p27 structures. Spy1 lacks the MRAIL binding cleft, present in CycA, into which p27 docks.

B p27 potently inhibits Cdk2-CycA but not Cdk2-Spy1. Kinase assay as in Fig 3 with 4 μM FoxM1 substrate and using full-length Spy1. Concentrations of p27 in each reaction are 0, 75, 150, 300, 600, 1,200, and 2,400 nM from left to right. Reported values are averages from three different experiments with the standard deviations shown as error bars.

C Crystal structure of the $p27^{KID}$-Cdk2-CycA ternary complex.

Source data are available online for this figure.

demonstrate that Spy1 lacks an intact p27-binding site and suggest that p27 poorly inhibits Cdk2-Spy1 activity. To test this hypothesis, we performed the ^{32}P-labeling reaction using FoxM1 substrate in the presence of increasing concentrations of the kinase inhibitory domain of p27 ($p27^{KID}$) (Fig 5B). $p27^{KID}$ potently inhibits Cdk2-CycA with a $K_i \sim 10$ nM. In contrast, $p27^{KID}$ shows little inhibition of Cdk2-Spy1 (full-length Spy1) even at concentrations ~1 μM, and our measurements fit a $K_i \sim 5$ μM.

Considering that Spy1 lacks the MRAIL binding cleft and that Cdk2 has been found in complexes with p27 and Spy1 in cells, we hypothesized that Cdk2 mediates the p27-Spy1 association within the ternary complex. We found by isothermal titration calorimetry that $p27^{KID}$ binds Cdk-Spy1 ($K_d = 180 \pm 70$ nM) (Fig EV3). This affinity is similar to that previously reported for Cdk2 alone and lower than the affinity for Cdk2-CycA ($K_d \sim 4$ nM) (Lacy *et al*, 2004). We crystallized the p27-Cdk2-Spy1 complex and determined

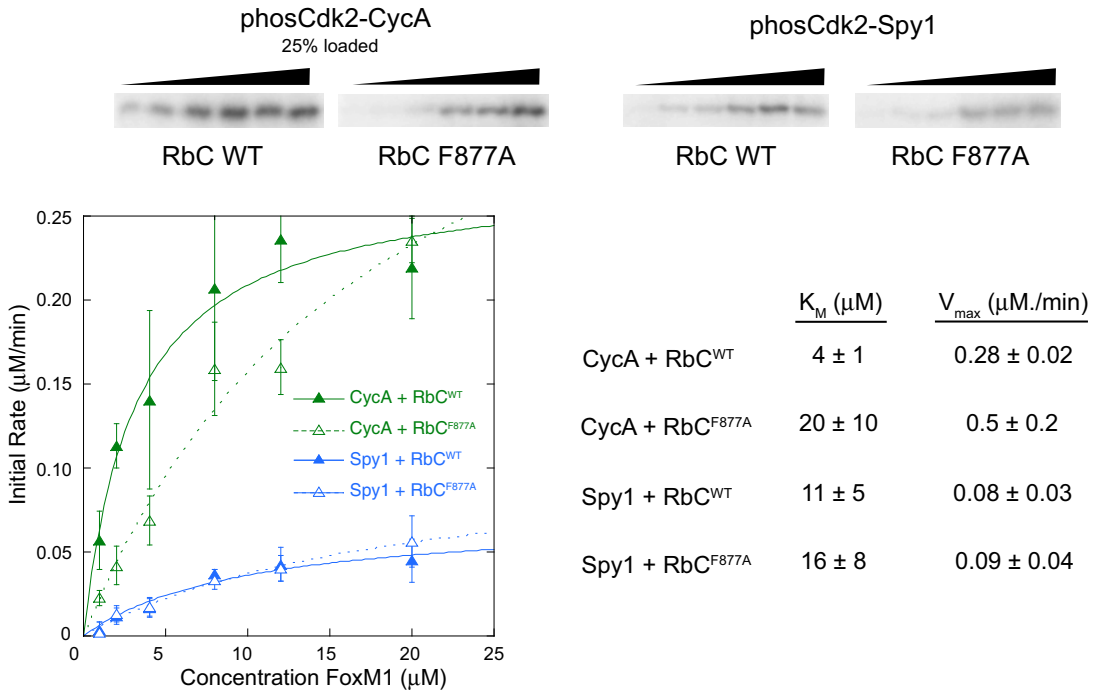

	K_M (μM)	V_{max} (μM./min)
CycA + RbC^{WT}	4 ± 1	0.28 ± 0.02
CycA + RbC^{F877A}	20 ± 10	0.5 ± 0.2
Spy1 + RbC^{WT}	11 ± 5	0.08 ± 0.03
Spy1 + RbC^{F877A}	16 ± 8	0.09 ± 0.04

Figure 6. Cdk2-Spy1 is less sensitive to the presence of a substrate-docking site than Cdk2-CycA.
Kinase assay as performed in Fig 3 but using full-length Spy1 and the Rb C-terminal domain (RbC, 7 consensus Cdk sites) as a substrate. F877A contains a mutation in the RxLF sequence that docks to the MRAIL site in CycA. Reported values are averages from three different experiments with the standard deviations shown as error bars. The kinetic parameters (with standard deviations reported as errors) averaged over the three replicates are shown in the table.
Source data are available online for this figure.

its structure to 3.5 Å (Table EV1 and Fig 5C). The structure of Spy1 in the ternary complex overlays well with its structure in the binary complex (RMSD = 0.436 Å). Electron density is only observable for p27 residues 51–91, which corresponds to the region that binds Cdk2. The structure of p27 in this region is similar to the structure of p27 bound to Cdk2-CycA (Russo *et al*, 1996a). Although present in the crystallization construct, the part of p27 that binds CycA in the ternary p27-Cdk2-CycA complex is not visible, which is consistent with the lack of a p27 binding site in the S/R box of Spy1. The structure of Cdk2 in the ternary complex with Spy1 overlays well with its structure in the ternary complex with CycA. The changes to the Cdk2 N-terminal lobe and insertion of p27 residues into the ATP binding site are consistent with an inactive kinase.

From these observations, we conclude that p27 binds the Cdk2-Spy1 complex weakly due to the lack of the MRAIL site, but when bound, p27 is capable of inhibiting Cdk2 as in the Cdk2-CycA-p27 complex. However, it is notable that our measured K_i of the p27^{KID} domain is ~25-fold weaker than the K_d that we measured for its association. We suggest that the bridging interaction p27 makes with both the kinase and CycA domains may play an additional role in inhibition, perhaps by restricting dynamics that are necessary for catalysis.

Substrate phosphorylation by Cdk2-Spy1 is not enhanced by cyclin-docking sequences

We also tested whether Cdk2-Spy1 was insensitive to the presence of the (R/K)xLxF motif in a substrate (Fig 6). We phosphorylated an Rb C-terminal domain construct (Rb$^{771–928}$, called RbC), which contains seven phosphorylation sites. RbC includes a KxLxF sequence that has been shown to be critical for Rb phosphorylation by Cdk-cyclin complexes *in vitro* and in cells (Adams *et al*, 1999; Hirschi *et al*, 2010). We compared Cdk2-CycA and Cdk2-Spy1 (full-length Spy1) in their ability to phosphorylate RbC and a mutant (F877A) in the KxLxF motif. In the steady-state kinetic assay with Cdk2-CycA, we find that V_{max}/K_M is sevenfold higher for RbC wild type than it is for RbC containing the F877A mutation. In contrast, in the reactions with Cdk2-Spy1, the V_{max}/K_M is similar for the substrates containing the wild-type and mutant docking site. These data indicate that substrate capture by Cdk2-CycA is more sensitive to the presence of the KxLxF site.

Discussion

Comparison of Spy1 and other cyclin-like proteins

The Cdk2-Spy1 structure reveals that the Cdk interaction surface of Spy1 resembles that of cyclin, particularly in the arrangement of the CBF helices (α3 and α5) that position the PSTAIRE helix in its active conformation (Fig 1B). While the primary sequence is not strictly conserved, the chemical nature of the residues responsible for Cdk interaction in this region is conserved. The remainder of the S/R box does not overlay well with cyclins, and there are important differences in how the Cdk T-loop is bound. These facts suggest that

Speedy and cyclins did not evolve from a common gene, but their evolution converged on a structure that activates Cdk. The active conformation of Cdk2 in the structure is consistent with our data confirming that S/R box-Cdk2 has activity and previous data that *Xenopus* S/R box alone is able to activate Cdk2 (Cheng *et al*, 2005a; Dinarina *et al*, 2005). It has been reported that the S/R box domain from mouse SpyA is not sufficient for Cdk2 activation (Cheng *et al*, 2005b); however, based on the domain boundaries in that study, we suggest that the expressed construct may have been too truncated and not stable.

Several examples of noncyclin proteins have been reported to positively regulate Cdk. For example, in neuronal cells, the protein p35 binds and activates Cdk5 (Dhavan & Tsai, 2001; Tarricone *et al*, 2001), and the protein Cks binds Cdk1 and Cdk2 to stimulate activity toward cell-cycle substrates phosphorylated at multiple sites (Pines, 1996; Koivomagi *et al*, 2013; McGrath *et al*, 2013). In organizing the active conformation of Cdk using a single CBF, Spy1 bares some similarities to how the neuron-specific noncanonical Cdk activator p35 binds Cdk5 and how the budding yeast activator Pho80 activates the Pho85 kinase (Tarricone *et al*, 2001; Huang *et al*, 2007). p35 binds and activates Cdk5 without the need for T-loop phosphorylation, and the T-loop conformations are similar in the Cdk2-Spy1 and Cdk5-p35 structures (Tarricone *et al*, 2001). However, the details of the Spy1-T-loop and p35-T-loop interactions are quite distinct, and there is overall poor conservation between Spy1 and p35 (Fig EV1).

Mechanism for Spy1-mediated Cdk2 activation

Our structure offers a clear explanation for why Cdk2 does not require T-loop phosphorylation for activity when bound by Spy1. Spy1 utilizes a set of conserved charged residues to bind the T-loop and pull it into its active conformation away from the Cdk2 substrate-binding site. We find that mutation of two of these residues (D97 and E135) results in loss of kinase activity and Spy1 function in driving cell proliferation and overriding DNA damage induced checkpoints (Fig 4). We observe no differences in the position of T14 and Y15 in the structure compared to the Cdk2-CycA complex, which is consistent with a report that Cdk2-Spy1 responds like Cdk2-CycA to inhibitory phosphorylation on these sites (Dinarina *et al*, 2005). Spy1 lacks the MRAIL binding cleft, which is present in cyclin and is accessed by protein Cdk inhibitors and substrates. Accordingly, we find that unlike Cdk2-CycA, Cdk2-Spy1 is not inhibited by p27 and does not show preference for substrates that contain RxLF-type docking motifs. Previous reports have demonstrated direct binding between Spy1 and p27 that depends on arginines within residues 170–180 of Spy1 (Porter *et al*, 2003; Al Sorkhy *et al*, 2016). In contrast, our structural data indicate that there is no direct interaction and that the association is mediated by Cdk. This discrepancy may be due to a role for the Spy1 C-terminal region that resides outside of the S/R box.

Our data are in agreement with previous reports that Cdk2-Spy1 activity toward consensus Cdk phosphorylation sites is not as efficient as phosCdk2-CycA when assaying purified proteins (Figs 3 and EV2) (Cheng *et al*, 2005a; Dinarina *et al*, 2005). Previous data demonstrate that while Cdk2-CycA prefers lysine or arginine at the +3 position of the phosphorylation site ((S/T)Px(K/R)), Cdk2-Spy1 tolerates most amino acid substitutions at the +3 position, preferring tyrosine, arginine, or tryptophan (Cheng *et al*, 2005a). Considering that the active site structures of the two complexes appear nearly identical, it is not clear why this difference is observed, but it may be due to subtle differences in affinity. We also note that the weaker Cdk2-Spy1 activity compared to Cdk2-CycA may be an artifact of the relative stabilities of the purified enzymes.

Roles of Spy1 in development and oncogenesis

Our data provide strong support for the hypothesis that Spy1 activates Cdk in a manner that is insensitive to many of the regulatory mechanisms that minimize Cdk activity. This insensitivity is likely important in the context of development, during which the cell cycle needs to progress in the presence of complex and potentially conflicting growth signals, and therefore, this hypothesis fits with observations that Spy1 is expressed in oocytes and the testes (Ferby *et al*, 1999; Porter *et al*, 2002; Cheng *et al*, 2005b; Mikolcevic *et al*, 2016). The insensitivity of Spy1 to antiproliferative signals may push stem cells past barriers at select time points during development as has been proposed in the brain (Lubanska *et al*, 2014).

Spy1 was originally isolated in two different screens designed to identify gene products capable of overriding cell-cycle checkpoints (Ferby *et al*, 1999; Lenormand *et al*, 1999). Spy1 has been shown to override cell-cycle checkpoints and apoptotic signaling and promote cell proliferation following a host of different forms of DNA damage (Barnes *et al*, 2003; McAndrew *et al*, 2009; Mikolcevic *et al*, 2016). As distinct hallmarks of cancer, this prompted the study of Spy1 in tumor initiation and promotion by a number of different research groups. Spy1 levels are high in hepatocellular carcinoma, lymphoma, malignant glioma, ovarian cancer, and breast cancer and knockdown of Spy1 protein significantly reduces tumorigenic capacity in numerous systems *in vivo* and *in vitro* (Golipour *et al*, 2008; Ke *et al*, 2009; Al Sorkhy *et al*, 2012; Hang *et al*, 2012; Zhang *et al*, 2012; Bisteau & Kaldis, 2014; Lubanska *et al*, 2014 Lu *et al*, 2016). These data suggest the possibility that Spy1 targeting may be a novel anticancer therapy. To date, targeting Cdk activity using Cdk inhibitors has had some clinical success (Stone *et al*, 2012; O'Leary *et al*, 2016); however, the roles of cyclin-like proteins have not been considered and information on how to best stratify patient populations for these studies is still accumulating. Our structural resolution of how Cdk is activated by Spy1, particularly the unique positioning of the Cdk T-loop, provides the foundation for developing Cdk-Spy1-specific kinase inhibitors that may have utility in the clinic.

Materials and Methods

Protein expression and purification

Wild-type human Spy1, S/R box (residues G61–D213), or CycA were each expressed as an MBP fusion protein from a codon-optimized sequence inserted into the pMBP vector in SoluBL21 *Escherichia coli*. Wild-type full-length human Cdk2 was expressed separately as a GST fusion protein from a pGEX vector in *E. coli*. In both cases, transformed cells were grown to an OD between 0.6 and 1, cooled in an ice bath for 20 min, and expression was induced with 1 mM IPTG overnight at 18°C. Cell pellets were

resuspended in a wash buffer containing 25 mM HEPES pH 7.5, 200 mM sodium chloride, 1 mM DTT. The resuspended cells from the separate batches of *E. coli* were lysed together with 1 mM PMSF to form the Cdk2-Spy1 (or Cdk2-CycA) complex. The clarified lysate was purified with glutathione Sepharose resin. The eluate from the glutathione Sepharose resin, which contained both Cdk2 and Spy1, was then bound to amylose resin and washed with the lysis buffer. The tags were then cleaved on-resin overnight with GST-TEV protease, and the GST-TEV and cleaved GST tag were separated from Cdk2-Spy1 complex with glutathione Sepharose. Trace amounts of cleaved MBP were separated from Cdk2-Spy1 complex with amylose resin. To express Cdk2 phosphorylated on T160, GST-tagged Cdk2 was coexpressed with yeast CAK from the pRSFduet vector in BL21 *E. coli*. Cdk2-CycA and Cdk2-Spy1 complexes for kinase assays were prepared without the cleavage of the tags. Tagged proteins were eluted from amylose resin with 1% maltose, mixed with glycerol (final 10% glycerol by volume), aliquoted, and flash-frozen in liquid nitrogen. Full-length human p27, the p27 kinase inhibitory domain ($p27^{KID}$, residues 22–93), and the FoxM1 and Rb proteins constructs were expressed as GST fusion proteins in *E. coli* and purified using affinity and anion exchange chromatography.

Crystallization and structure determination

The Cdk2-Spy1 (S/R box) complex was subjected to limited proteolysis with 0.01% trypsin for 30 min on ice. The trypsinized complex appeared on a denaturing gel as a stable band with a small decrease in mass. After trypsinizing, Cdk2-Spy1 complex was prepared for crystallization by final purification using a HiLoad Superdex 200 (GE Healthcare) column equilibrated in a buffer containing 12.5 mM HEPES pH 7.5, 150 mM NaCl, and 1 mM TCEP. The final concentration of protein complex used for purification was 5 mg/ml. Proteins were crystallized by sitting-drop vapor diffusion at 20°C. Two different crystal forms were grown for 4 weeks. An initial dataset was collected from a crystal grown in 1 M lithium chloride, 12% PEG 6000, and 0.1 M MES pH 6.2, harvested and flash-frozen in the same solution with 20% PEG 200. A second data set was collected from a crystal grown in a solution containing 900 mM potassium sodium tartrate, 200 mM lithium sulfate, and 0.1 M CHES pH 9.3. The crystals were harvested and flash-frozen in the same solution with 15% glycerol.

The Cdk2-Spy1-p27 ternary complex was assembled from the S/R box of human Spy1A, full-length Cdk2, and full-length p27. Purified p27 was mixed in slight stoichiometric excess with Cdk2-Spy1 following purification of the dimer over Superdex 200. The ternary complex was then purified to 11.5 mg/ml. Crystals of the ternary complex were grown by sitting-drop vapor diffusion at 20°C in 5% PEG 6000 and 0.1 M MES pH 5, harvested and flash-frozen in 20% PEG 200.

Data were collected at λ = 1.0332 Å, 100 K on Beamline 23-ID-D at the Advanced Photon Source, Argonne National Laboratory. Diffraction spots were integrated with Mosflm (Leslie, 2006) and scaled with SCALE-IT (Howell & Smith, 1992). Phases were solved by molecular replacement with PHASER (Mccoy *et al*, 2007). CDK2 (PDB: 1QMZ) was used as a search model to solve the first data set ($P3_121$ crystal form, grown in PEG 6000). The initial model was rebuilt with Coot (Emsley & Cowtan, 2004), and Speedy was added to the unmodeled electron density. The resulting model was refined with Phenix (Adams *et al*, 2010). Several rounds of position refinement with simulated annealing and individual temperature-factor refinement with default restraints were applied. The second data set ($P3_121$ crystal form, grown in sodium tartrate) and the data set for the ternary complex crystal were collected and processed as above. Both structures were solved by molecular replacement using the structure from the first binary complex crystal as a search model. The final refined models were deposited in the Protein Data Bank under Accession Codes 5UQ1, 5UQ2, and 5UQ3.

Kinase assays

Kinase reactions were performed in a volume of 100 µl in a buffer containing 25 mM HEPES, 200 mM NaCl, 10 mM $MgCl_2$, 1 mM DTT, 200 µM ATP, and 100 µCi of ^{32}P-γ-ATP (pH 7.0). Substrate was diluted into the reaction buffer at the appropriate concentration, and the reaction was initiated through addition of kinase. Reactions were quenched after 10 min though addition of SDS–PAGE loading buffer. Independent time course experiments confirmed that phosphate addition is still linear with time beyond 30 min using our experimental conditions. Electrospray mass spectrometry confirmed that under conditions that drive the kinase reactions to completion (near stoichiometric concentrations of kinase) 5 and 7 phosphates are incorporated into FoxM1 and RbC, respectively. Such a stoichiometric reaction was performed with each ^{32}P-assay, and the band from the quantitatively phosphorylated substrate was used as a standard to calculate phosphate concentration from band intensity. This phosphate concentration was then used to determine initial rate of phosphate incorporation. SDS–PAGE gels were imaged with a Typhoon scanner and bands quantified using the ImageJ software package. For each assay, three replicates were performed. The kinetic parameters (K_M, V_{max}, K_i) were determined for each individual replicate, and the reported values are averages of the three replicates with standard deviations reported as errors. The data points and error bars shown in the figure graphs are the averages and standard deviations, respectively, of initial rates at each concentration point across the three replicates.

Isothermal titration calorimetry

ITC was performed using a MicroCal VP-ITC calorimeter. Cdk2-Spy1 S/R box and p27 KID were buffer exchange over Superdex 200 into 20 mM HEPES (pH 7.5), 200 mM NaCl, and 5 mM DTT. p27 at concentrations between 100 and 270 µM was titrated into Cdk2-Spy1 S/R box at concentrations between 14 and 25 µM. Data were analyzed with the Origin calorimetry software package assuming a one-site binding model. Experiments were performed in triplicate, and the reported error is the standard deviation of each set of measurements.

Cell culture assays

The pCS3 and Myc-Spy1-pCS3 vectors were generated as previously described (Porter *et al*, 2002). Site-directed mutagenesis was performed to create the Myc-Spy1-D97N/E135Q-pCS3 vector. HEK-293 and NIH 3T3 cells were cultured in Dulbecco's modified Eagle's medium (DMEM) with 10% fetal bovine serum and 1% penicillin/streptomycin at 37°C and 5% CO_2. Transient transfection of HEK-293 cells was conducted using 25 µg of polyethylenimine (PEI) and

10 μg of DNA. DNA and PEI were incubated for 10 min at room temperature in base medium before added to the plate. The transfection reagent was removed after 16–18 h. Transient transfection of NIH 3T3 cells required 10 μg of DNA and 30 μg of PEI to 500 μl of 1× PBS, vortexed briefly, and allowed to incubate for 10 min at room temperature. Just prior to addition of the DNA PEI complex, the media on the plate was changed to two-thirds serum free media and one-third 1× PBS. The DNA PEI complex was added to the cells and incubated at 37°C 5% CO_2 for 4 h. After 4 h, the media was changed to full growth media.

Transfection was monitored using quantitative real-time (qRT)–PCR. RNA was isolated using Qiagen RNeasy Kit following manufacturer's instructions. Equal amounts of cDNA were synthesized using qScript cDNA SuperMix following manufacturer's instructions. qRT–PCR was performed using SYBR Green Detection (Applied Biosystems) and was analyzed using the Viia6 Real-Time PCR System (Life Technologies) and software.

Cell proliferation assays were conducted by seeding cells in a 24-well plate at a density of 15,000 cells per well. Trypan blue exclusion analysis was used to determine cell viability at 5 days postseeding and assess rates of proliferation.

Expanded View for this article is available online.

Acknowledgements
This research used resources of the Advanced Photon Source, beamline 23-ID-B, a U.S. Department of Energy (DOE) Office of Science User Facility operated for the DOE Office of Science by Argonne National Laboratory under Contract No. DE-AC02-06CH11357. This work was supported by the Paul and Anne Irwin Graduate Fellowship in Cancer Research to D.A.M., a scholarship from the Canadian Breast Cancer Foundation to B.F., a grant from the Canadian Institutes of Health Research to L.A.P, and grants from the National Institutes of Health (R01CA132685) and American Cancer Society (RSG-12-131-01-CCG) to S.M.R.

Author contributions
DAM, B-AF, LAP, and SMR designed experiments and wrote the manuscript. DAM, B-AF, AHM, and ST performed experiments. All authors analyzed experiments and reviewed the manuscript.

Conflict of interest
The authors declare that they have no conflict of interest.

References

Adams PD, Li X, Sellers WR, Baker KB, Leng X, Harper JW, Taya Y, Kaelin WG Jr (1999) Retinoblastoma protein contains a C-terminal motif that targets it for phosphorylation by cyclin-cdk complexes. *Mol Cell Biol* 19: 1068 – 1080

Adams PD, Afonine PV, Bunkoczi G, Chen VB, Davis IW, Echols N, Headd JJ, Hung LW, Kapral GJ, Grosse-Kunstleve RW, McCoy AJ, Moriarty NW, Oeffner R, Read RJ, Richardson DC, Richardson JS, Terwilliger TC, Zwart PH (2010) PHENIX: a comprehensive Python-based system for macromolecular structure solution. *Acta Crystallogr D Biol Crystallogr* 66: 213 – 221

Al Sorkhy M, Craig R, Market B, Ard R, Porter LA (2009) The cyclin-dependent kinase activator, Spy 1A, is targeted for degradation by the ubiquitin ligase NEDD4. *J Biol Chem* 284: 2617 – 2627

Al Sorkhy M, Ferraiuolo RM, Jalili E, Malysa A, Fratiloiu AR, Sloane BF, Porter LA (2012) The cyclin-like protein Spy1/RINGO promotes mammary transformation and is elevated in human breast cancer. *BMC Cancer* 12: 45

Al Sorkhy M, Fifield BA, Myers D, Porter LA (2016) Direct interactions with both p27 and Cdk2 regulate Spy1-mediated proliferation *in vivo* and *in vitro*. *Cell Cycle* 15: 128 – 136

Barnes EA, Porter LA, Lenormand JL, Dellinger RW, Donoghue DJ (2003) Human Spy1 promotes survival of mammalian cells following DNA damage. *Cancer Res* 63: 3701 – 3707

Bisteau X, Kaldis P (2014) Spy1/SpeedyA accelerates neuroblastoma. *Oncotarget* 5: 6554 – 6555

Brown NR, Noble ME, Endicott JA, Johnson LN (1999) The structural basis for specificity of substrate and recruitment peptides for cyclin-dependent kinases. *Nat Cell Biol* 1: 438 – 443

Cheng A, Gerry S, Kaldis P, Solomon MJ (2005a) Biochemical characterization of Cdk2-Speedy/Ringo A2. *BMC Biochem* 6: 19

Cheng A, Xiong W, Ferrell JE, Solomon MJ (2005b) Identification and comparative analysis of multiple mammalian Speedy/Ringo proteins. *Cell Cycle* 4: 155 – 165

Debondt HL, Rosenblatt J, Jancarik J, Jones HD, Morgan DO, Kim SH (1993) Crystal-structure of cyclin-dependent kinase-2. *Nature* 363: 595 – 602

Dhavan R, Tsai LH (2001) A decade of CDK5. *Nat Rev Mol Cell Biol* 2: 749 – 759

Dinarina A, Perez LH, Davila A, Schwab M, Hunt T, Nebreda AR (2005) Characterization of a new family of cyclin-dependent kinase activators. *Biochem J* 386: 349 – 355

Emsley P, Cowtan K (2004) Coot: model-building tools for molecular graphics. *Acta Crystallogr D Biol Crystallogr* 60: 2126 – 2132

Ferby I, Blazquez M, Palmer A, Eritja R, Nebreda AR (1999) A novel p34(cdc2)-binding and activating protein that is necessary and sufficient to trigger G (2)/M progression in *Xenopus oocytes*. *Genes Dev* 13: 2177 – 2189

Gastwirt RF, Slavin DA, McAndrew CW, Donoghue DJ (2006) Spy1 expression prevents normal cellular responses to DNA damage: inhibition of apoptosis and checkpoint activation. *J Biol Chem* 281: 35425 – 35435

Golipour A, Myers D, Seagroves T, Murphy D, Evan GI, Donoghue DJ, Moorehead RA, Porter LA (2008) The Spy1/RINGO family represents a novel mechanism regulating mammary growth and tumorigenesis. *Cancer Res* 68: 3591 – 3600

Hang QL, Fei M, Hou SC, Ni QC, Lu CH, Zhang GW, Gong PP, Guan CQ, Huang XT, He S (2012) Expression of Spy1 protein in human Non-Hodgkin's Lymphomas is correlated with phosphorylation of p27(Kip1) on Thr187 and cell proliferation. *Med Oncol* 29: 3504 – 3514

Hirschi A, Cecchini M, Steinhardt RC, Schamber MR, Dick FA, Rubin SM (2010) An overlapping kinase and phosphatase docking site regulates activity of the retinoblastoma protein. *Nat Struct Mol Biol* 17: 1051 – 1057

Howell PL, Smith GD (1992) Identification of heavy-atom derivatives by normal probability methods. *J Appl Crystallogr* 25: 81 – 86

Huang K, Ferrin-O'Connell I, Zhang W, Leonard GA, O'Shea EK, Quiocho FA (2007) Structure of the Pho85-Pho80 CDK-cyclin complex of the phosphate-responsive signal transduction pathway. *Mol Cell* 28: 614 – 623

Jeffrey PD, Ruso AA, Polyak K, Gibbs E, Hurwitz J, Massague J, Pavletich NP (1995) Mechanism of Cdk activation revealed by the structure of a CyclinA-Cdk2 complex. *Nature* 376: 313 – 320

Karaiskou A, Perez LH, Ferby I, Ozon R, Jessus C, Nebreda AR (2001) Differential regulation of Cdc2 and Cdk2 by RINGO and cyclins. *J Biol Chem* 276: 36028 – 36034

Ke Q, Ji JL, Cheng C, Zhang YX, Lu MD, Wang Y, Zhang L, Li P, Cui XP, Chen L, He S, Shen AG (2009) Expression and prognostic role of Spy1 as a novel cell cycle protein in hepatocellular carcinoma. *Exp Mol Pathol* 87: 167 – 172

Kim WY, Sharpless NE (2006) The regulation of INK4/ARF in cancer and aging. *Cell* 127: 265 – 275

Koivomagi M, Ord M, Iofik A, Valk E, Venta R, Faustova I, Kivi R, Balog ER, Rubin SM, Loog M (2013) Multisite phosphorylation networks as signal processors for Cdk1. *Nat Struct Mol Biol* 20: 1415 – 1424

Lacy ER, Filippov I, Lewis WS, Otieno S, Xiao L, Weiss S, Hengst L, Kriwacki RW (2004) p27 binds cyclin-CDK complexes through a sequential mechanism involving binding-induced protein folding. *Nat Struct Mol Biol* 11: 358 – 364

Laoukili J, Alvarez M, Meijer LA, Stahl M, Mohammed S, Kleij L, Heck AJ, Medema RH (2008) Activation of FoxM1 during G2 requires cyclin A/Cdk-dependent relief of autorepression by the FoxM1 N-terminal domain. *Mol Cell Biol* 28: 3076 – 3087

Lenormand JL, Dellinger RW, Knudsen KE, Subramani S, Donoghue DJ (1999) Speedy: a novel cell cycle regulator of the G2/M transition. *EMBO J* 18: 1869 – 1877

Leslie AG (2006) The integration of macromolecular diffraction data. *Acta Crystallogr D Biol Crystallogr* 62: 48 – 57

Lu SM, Liu R, Su M, Wei YZ, Yang SY, He S, Wang X, Qiang FL, Chen C, Zhao SY, Zhang WW, Xu P, Mao GX (2016) Spy1 participates in the proliferation and apoptosis of epithelial ovarian cancer. *J Mol Histol* 47: 47 – 57

Lubanska D, Market-Velker BA, deCarvalho AC, Mikkelsen T, Fidalgo da Silva E, Porter LA (2014) The cyclin-like protein Spy1 regulates growth and division characteristics of the $CD133^+$ population in human glioma. *Cancer Cell* 25: 64 – 76

Major ML, Lepe R, Costa RH (2004) Forkhead box M1B transcriptional activity requires binding of Cdk-cyclin complexes for phosphorylation-dependent recruitment of p300/CBP coactivators. *Mol Cell Biol* 24: 2649 – 2661

Malumbres M, Barbacid M (2009) Cell cycle, CDKs and cancer: a changing paradigm. *Nat Rev Cancer* 9: 153 – 166

McAndrew CW, Gastwirt RF, Meyer AN, Porter LA, Donoghue DJ (2007) Spy1 enhances phosphorylation and degradation of the cell cycle inhibitor p27. *Cell Cycle* 6: 1937 – 1945

McAndrew CW, Gastwirt RF, Donoghue DJ (2009) The atypical CDK activator Spy1 regulates the intrinsic DNA damage response and is dependent upon p53 to inhibit apoptosis. *Cell Cycle* 8: 66 – 75

Mccoy AJ, Grosse-Kunstleve RW, Adams PD, Winn MD, Storoni LC, Read RJ (2007) Phaser crystallographic software. *J Appl Crystallogr* 40: 658 – 674

McGrath DA, Balog ER, Koivomagi M, Lucena R, Mai MV, Hirschi A, Kellogg DR, Loog M, Rubin SM (2013) Cks confers specificity to phosphorylation-dependent CDK signaling pathways. *Nat Struct Mol Biol* 20: 1407 – 1414

Mikolcevic P, Isoda M, Shibuya H, Barrantes ID, Igea A, Suja JA, Shackleton S, Watanabe Y, Nebreda AR (2016) Essential role of the Cdk2 activator RingoA in meiotic telomere tethering to the nuclear envelope. *Nat Commun* 7: 11084 – 11097

Morgan DO (2007) *The cell cycle: principles of control*. London; Sunderland, MA: Published by New Science Press in Association with Oxford University Press; Distributed Inside North America by Sinauer Associates Publishers

Nebreda AR (2006) CDK activation by non-cyclin proteins. *Curr Opin Cell Biol* 18: 192 – 198

Noble MEM, Endicott JA, Brown NR, Johnson LN (1997) The cyclin box fold: protein recognition in cell-cycle and transcription control. *Trends Biochem Sci* 22: 482 – 487

O'Leary B, Finn RS, Turner NC (2016) Treating cancer with selective CDK4/6 inhibitors. *Nat Rev Clin Oncol* 13: 417 – 430

Pines J (1996) Cell cycle: reaching for a role for the Cks proteins. *Curr Biol* 6: 1399 – 1402

Porter LA, Dellinger RW, Tynan JA, Barnes EA, Kong M, Lenormand JL, Donoghue DJ (2002) Human speedy: a novel cell cycle regulator that enhances proliferation through activation of Cdk2. *J Cell Biol* 157: 357 – 366

Porter LA, Kong-Beltran M, Donoghue DJ (2003) Spy1 interacts with p27Kip1 to allow G1/S progression. *Mol Biol Cell* 14: 3664 – 3674

Russo AA, Jeffrey PD, Patten AK, Massague J, Pavletich NP (1996a) Crystal structure of the p27(Kip1) cyclin-dependent-kinase inhibitor bound to the cyclin A Cdk2 complex. *Nature* 382: 325 – 331

Russo AA, Jeffrey PD, Pavletich NP (1996b) Structural basis of cyclin-dependent kinase activation by phosphorylation. *Nat Struct Biol* 3: 696 – 700

Schulman BA, Lindstrom DL, Harlow E (1998) Substrate recruitment to cyclin-dependent kinase 2 by a multipurpose docking site on cyclin A. *Proc Natl Acad Sci USA* 95: 10453 – 10458

Sherr CJ, Roberts JM (1995) Inhibitors of mammalian G1 cyclin-dependent kinases. *Genes Dev* 9: 1149 – 1163

Sherr CJ (1996) Cancer cell cycles. *Science* 274: 1672 – 1677

Stone A, Sutherland RL, Musgrove EA (2012) Inhibitors of cell cycle kinases: recent advances and future prospects as cancer therapeutics. *Crit Rev Oncog* 17: 175 – 198

Swanton C, Mann DJ, Fleckenstein B, Neipel F, Peters G, Jones N (1997) Herpes viral cyclin/Cdk6 complexes evade inhibition by CDK inhibitor proteins. *Nature* 390: 184 – 187

Tarricone C, Dhavan R, Peng JM, Areces LB, Tsai LH, Musacchio A (2001) Structure and regulation of the CDK5-p25(nck5a) complex. *Mol Cell* 8: 657 – 669

Zhang L, Shen AG, Ke Q, Zhao W, Yan MJ, Cheng C (2012) Spy1 is frequently overexpressed in malignant gliomas and critically regulates the proliferation of glioma cells. *J Mol Neurosci* 47: 485 – 494

